JACS
JOURNAL OF THE AMERICAN CHEMICAL SOCIETY
pubs.acs.org/JACS
Article

Dark State of the Thiele Hydrocarbon: Efficient Solvatochromic Emission from a Nonpolar Centrosymmetric Singlet Diradicaloid

Angela Punzi,[#] Yasi Dai,[#] Carlo N. Dibenedetto, Ernesto Mesto, Emanuela Schingaro, Tobias Ullrich, Marinella Striccoli, Dirk M. Guldi,* Fabrizia Negri,* Gianluca M. Farinola,* and Davide Blasi*

Cite This: J. Am. Chem. Soc. 2023, 145, 20229−20241

Read Online

ACCESS | Metrics & More | Article Recommendations | Supporting Information

ABSTRACT: In this work, a comprehensive investigation of the photoinduced processes and mechanisms linked to the luminescence of a novel nonperchlorinated Thiele hydrocarbon (**TTH**) is presented. Despite the comparable diradical character of **TTH** (y_0 = 0.32−0.44) and the unsubstituted Thiele hydrocarbon (**TH**) (y_0 = 0.30), the polyhalogenated species is inert and photostable, showing an intense deep-red/near-infrared (NIR) fluorescence (photoluminescence quantum yield (PLQY) = 0.84 in toluene) even at room temperature and in the solid state (PLQY = 0.19). **TTH** displays a large Stokes shift (307 nm in benzonitrile) and solvatochromic behavior, which is unusual for a centrosymmetric, nonpolar, and low-conjugated species. These outstanding emission features are interpreted through quantum-chemical calculations, indicating that its fluorescence arises from the low-lying dark doubly excited zwitterionic state, typically found at low excitation energies in diradicaloids, acquiring dipole moment and intensity by state mixing *via* twisting around the strongly elongated exocyclic CC bonds of the excited *p*-quinodimethane (*p*QDM) core, with a mechanism similar to sudden polarization occurring in olefins. Such a mechanism is derived from ns and fs transient absorption measurements.

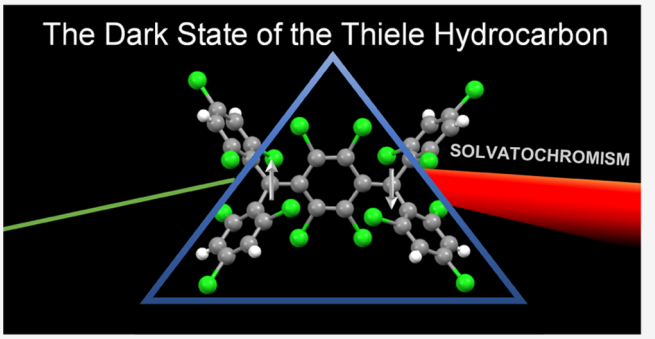

Downloaded via UNIV BOLOGNA on October 15, 2023 at 19:55:54 (UTC).
See https://pubs.acs.org/sharingguidelines for options on how to legitimately share published articles.

INTRODUCTION

Singlet diradicaloids (SDs) are emerging as a promising class of molecular materials due to their potential multiple applications in several fields.[1,2] Many examples of SDs have been reported as conductive materials,[3,4] semiconductors in organic field-effect transistors (OFETs),[5−8] singlet-fission species for organic photovoltaics (OPV),[9−11] near-infrared (NIR)-absorbing chromophores, and dyes for nonlinear optics (NLO).[12,13] A widely underestimated property of these versatile compounds is their luminescence.[11,14−16] This is quite surprising since the first-ever synthesized SD, the Thiele hydrocarbon (**TH**) (Figure 1),[17] was described as fluorescent in solution and slightly oxygen- and light-sensitive.[18] Probably, its photosensitivity and essentially quinoidal ground-state configuration limited the interest in the luminescence properties owned by the simplest *para*-quinodimethane (*p*QDM) diradicaloid. Actually, most of the synthetic efforts for developing new and stable **TH** derivatives were focused on the enhancement of the diradical character (described with the diradical index y_0, ranging from zero to one, moving from a closed-shell species to a pure diradical)[19] and mainly consisted in the introduction of heteroatoms in the **TH** backbone and the extension of the π-system.[20−25] However, the luminescence arising from open-shell species is currently being intensively investigated, focusing on the development of highly fluorescent polyhalogenated trityl radicals.[26] **TTM** and **PTM** (Figure 1) adducts have been proficiently used as functional units in several molecular materials for NLO,[27,28] circularly polarized luminescence (CPL),[29−31] magnetoluminescence,[32,33] and electroluminescence.[34,35] In particular, **TTM** was the first polyhalogenated triaryl radical exhibiting excimer emission when dispersed into rigid hosts,[36] while its push−pull derivatives led to a record device performance when used as emitters in organic light-emitting diodes (OLEDs), reaching the physical limit of 100% of internal quantum efficiency.[37] The key for this success is their extraordinary stability, mainly ensured by the six ortho chlorine atoms, which exert a shielding effect on the odd electron localized on the *ipso*-C.[38] Interestingly, perchlorination was already used as a synthetic approach for the stabilization of *p*QDM diradicaloids.[39,40] In 1991, Castañer et al. reported the synthesis and characterization of the perchlorinated Thiele hydrocarbon (**PTH**) (Figure 1).[40] The authors expected that the twist induced by

Received: October 6, 2022
Published: September 6, 2023

© 2023 American Chemical Society

https://doi.org/10.1021/jacs.3c05251
J. Am. Chem. Soc. 2023, 145, 20229−20241

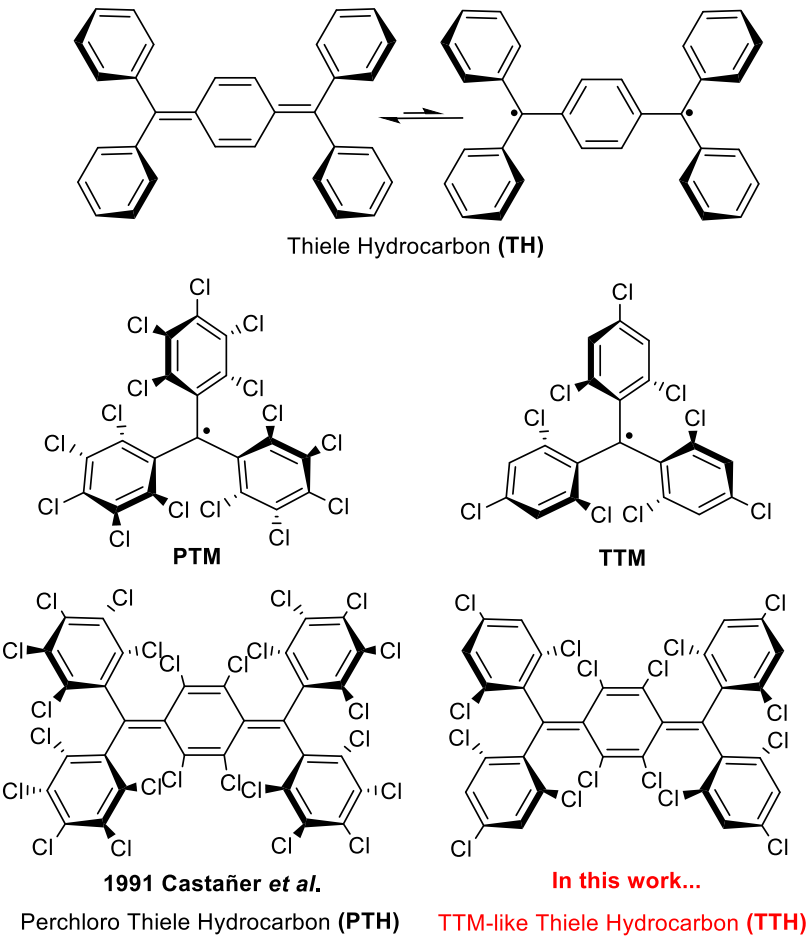

Figure 1. Molecular structures of Thiele hydrocarbon (**TH**), **PTM** and **TTM** radicals, perchloro Thiele hydrocarbon (**PTH**), and **TTM**-like Thiele hydrocarbon (**TTH**).

Scheme 1. Reaction Scheme for the Synthesis of TTH

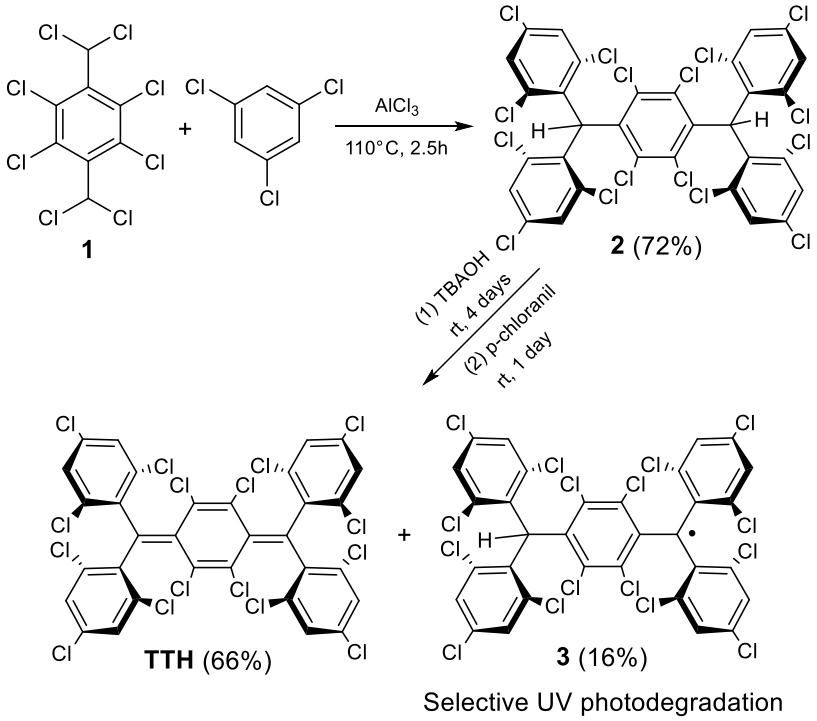

https://doi.org/10.1021/jacs.3c05251
J. Am. Chem. Soc. 2023, 145, 20229−20241

the bulky chlorine atoms near the exocyclic double bonds of the perchlorinated *p*-xylylene bridge would favor a triplet electronic configuration. In contrast, the electron paramagnetic resonance (EPR) and UV−vis characterizations depicted a quinoidal structure consistent with the one of the unsubstituted **TH**. A further study by Domingo et al. focused instead on the internal charge-transfer (ICT) properties of the **PTH** mixed-valence compound (anion-radical).[41] Oddly, both works did not mention any luminescence feature for the perchlorinated diradicaloid. Based on these findings, we synthesized a novel **TTM**-like Thiele hydrocarbon (**TTH**) (Figure 1), namely, 2,2′,2″,2‴-((perchlorocyclohexa-2,5-diene-1,4-diyliene)bis(methanediylyldene))tetrakis-(1,3,5-trichlorobenzene), aiming to obtain a highly fluorescent and inert *p*QDM diradicaloid, suitable to be easily characterized and processed. In fact, in analogy with what is already reported for polyhalogenated trityl radicals, **TTM** derivatives exhibit superior photoluminescence quantum yields (PLQYs) compared with **PTM** ones.[34,42] This aspect, together with the elevated molecular rigidity of **TTH** given by the coexistence of exocyclic double bonds and ortho halogens, should guarantee high values of PLQY. Moreover, the absence of chlorine atoms in meta positions undeniably affects the molecule processability, improving its solubility and favoring the thermal evaporation. The interest in the synthesis of highly fluorescent *p*QDM diradicaloids goes beyond their possible applications in optoelectronics or NLO[43,44] since the study of their luminescence can provide new fundamental insights into the nature of the emitting excited state[14,45] and its correlation with the ground-state open-shell character.[46] Furthermore, their diradical character is attracting much interest for the possibility of controlling spin states through conformational changes.[47−49]

RESULTS AND DISCUSSION

Synthesis and Purification. **TTH** was synthesized with a similar procedure to the one used for **PTH**, and its synthesis is briefly described in Scheme 1 (details in the Supporting Information (SI)). An excess of tetrabutylammonium hydroxide (TBAOH) was used for the conversion of **2** into the dianionic species. Then, after oxidation with *p*-chloranil, a mixture of **TTH** and monoradical **3** was obtained.[50] The radical nature of **3** was suggested by the presence of an intense absorption band at 382 nm, typical of polychlorinated trityl radicals (Figure 2a),[36] and was confirmed by high-resolution mass analysis (data not shown). It was not possible to purify the product *via* crystallization or through column chromatography on silica gel since both species showed almost the same retention factor. Therefore, to isolate **TTH**, its exceptional photostability was exploited. In fact, polyhalogenated trityl radicals such as **TTM** (Figure 1) suffer from severe photosensitivity (Figure 2b), which is usually reduced by coupling the radical core that behaves as an electron-acceptor (A) moiety with an electron-donor (D) group, generating, in this way, a push−pull derivative.[51−53] As in the case of **TTM**, the impurity **3** behaved as a photosensitive species due to the lack of a charge-transfer stabilization of the radical. The absorption spectrum in $CHCl_3$ of a mixed fraction containing both **TTH** and **3**, before and after irradiation with a UV lamp at 365 nm, is shown in Figure 2a. The absorption band at 382 nm belonging to **3** was rapidly quenched, while the band at 502 nm of **TTH** remained almost unaffected by the prolonged photoexcitation. After the complete photodegradation of **3**, **TTH** was easily isolated through column chromatography on silica gel (see the SI).

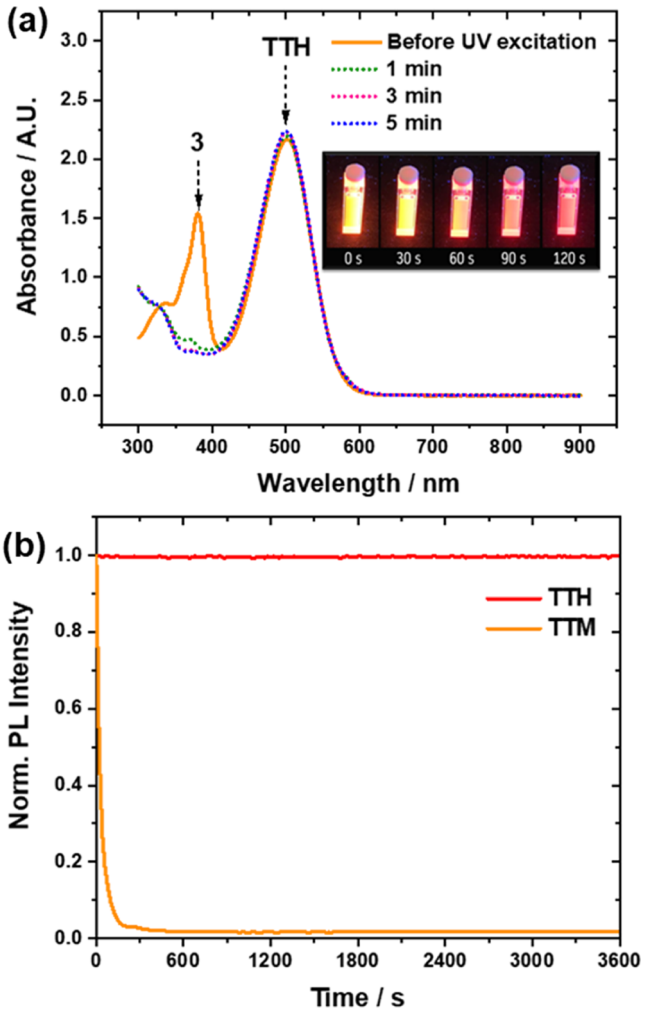

Figure 2. (a) Absorption spectrum of a $CHCl_3$ solution containing the monoradical impurity **3** and **TTH** (fraction obtained after the first column chromatography purification; see the SI) before and after continuous irradiation with UV light at 365 nm; inset: photographs of the same solution at different times under continuous UV irradiation, showing the fast photobleaching of **3** (yellow emitting species). (b) Normalized PL photobleaching of **TTH** (red) and **TTM** (orange) in $CHCl_3$ under continuous irradiation at 365 nm.

Single Crystal X-ray Diffraction (SCXRD). Crystals of **TTH** suited for SCXRD were obtained by dissolving a few mg of the compound in 1 mL of CH_2Cl_2, followed by the dropwise addition of 1 mL of hexane and leaving the solvent to slowly evaporate. SCXRD preliminary screening of several crystals of **TTH** evidenced that most of them showed a poor diffracting behavior. The best crystal was selected for the data acquisition that was measured with a 0.9 Å resolution. The Oak Ridge thermal ellipsoid plot (ORTEP) view of the crystal structure, as derived from the structural refinement, is given in Figure 3a, and the selected bond distances and bond angles are listed in Figure 3b and Table 1, respectively. SCXRD analysis confirmed the formation of the molecule that crystallizes in the $P2_1$ space group (Table S1). It exhibits two atropoisomeric centers located at C4 and C20 sp^2-carbon atoms having Minus (M) and Plus (P) conformations, respectively, depending on the left- or right-handed torsion of phenyl rings.[30,31] Similar to

https://doi.org/10.1021/jacs.3c05251
J. Am. Chem. Soc. 2023, 145, 20229−20241

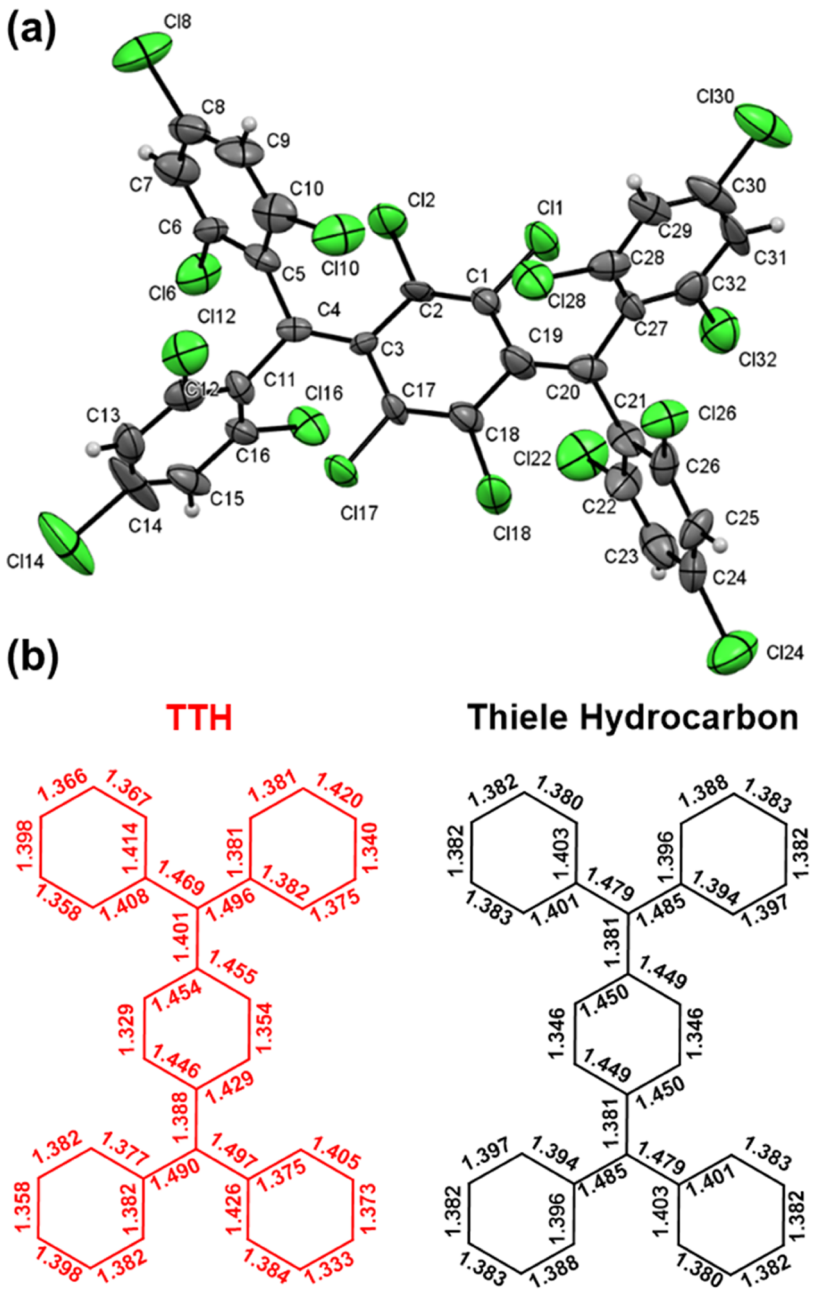

Figure 3. (a) ORTEP view of **TTH** that shows the atom-numbering scheme employed. For the sake of clarity, the hydrogen labels are omitted. (b) Comparison of the bond lengths in **TTH** and **TH.**[18]

Table 1. Selected Bond Angles for TTH and TH

A–B–C	angle **TTH** (deg)	angle **TH** (deg)[18]
C3–C4–C5	120.3	122.9
C19–C20–C21	121.9	122.9
C3–C4–C11	122.3	121.6
C19–C20–C27	123.8	121.6

the structure of **TH**, there is a well-defined bond length alternation in the *p*-xylylene framework, consistent with a quinoidal configuration.[18] The quinoidal structure agrees with the density functional theory (DFT)-computed ground-state geometry (Figure S12), displaying a moderate diradical character with y_0(PUHF) values computed in the range 0.32–0.44, only slightly larger than the diradical character of **TH** (y_0(PUHF) = 0.30).

The terminal C4 and C20 carbons of the *p*-xylylene system deviate from coplanarity (calculated deviation of 0.15(1) and 0.11(1) Å, respectively). Specifically, the C2–C3–C4–C5, C11–C4–C3–C17, C1–C19–C20–C27, and C18–C19–C20–C21 torsion angles are about 37, 29, 26, and 30°, respectively, in good agreement with the computed DFT dihedral angles of 25 and 26° (Figure S13a). Notably, the trityl propellers of **TTH** are less tilted compared to the analogous ones of **TTM** and **PTM** radicals.[54,55] Specifically, for **PTM**, an average torsion angle of 51° is reported, while for **TTM**, the average torsion angle is 47°. In addition, because of the steric interactions between the *p*-xylylene bridge and the phenyl groups, the latter are displaced out of the main plane of the molecule. The C3–C4 and C19–C20 bond lengths are close to those expected for olefin systems.

https://doi.org/10.1021/jacs.3c05251
J. Am. Chem. Soc. 2023, 145, 20229–20241

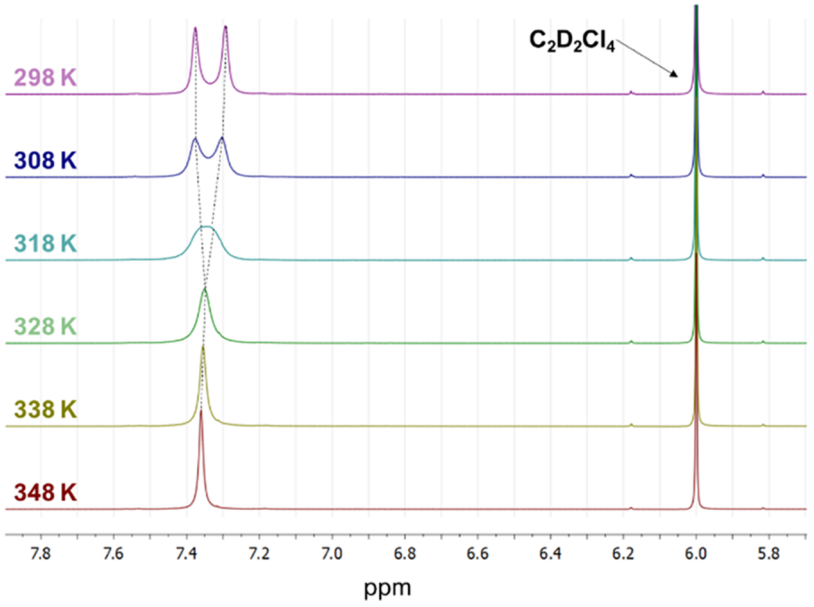

Figure 4. ^{1}H NMR spectra of **TTH** in $C_2D_2Cl_4$ varying the temperature in the range 298−348 K.

High-Temperature ^{1}H NMR Characterization. The quinoidal structure of **TTH** was confirmed by ^{1}H NMR characterization, performed in deuterated 1,1,2,2-tetrachloroethane ($C_2D_2Cl_4$) by varying the temperature in the 298−348 K range. As can be seen in Figure 4, no thermal-accessible triplet states were detected on increasing the temperature, while the temperature effect on the free rotation of phenyl substituents was clearly seen. In fact, while at 298 K the spectrum displayed two singlets at 7.37 and 7.29 ppm, due to steric restrictions to the free rotation of phenyl substituents (confirming the high rigidity of the molecule at room temperature), starting from 328 K these signals coalesced to a single peak at 7.36 ppm, indicating their free rotation. Beyond its impressive photostability, **TTH** showed an elevated thermal stability, compatible with thermal evaporation processing. The thermogravimetric analysis (TGA) in a nitrogen atmosphere displayed no degradation up to ∼330 °C (Figure S8), a lower value compared with **PTH**, for which a temperature of 395 °C was reported.[40] A similar behavior is seen for polyhalogenated trityl radicals, for which their thermal stability is directly correlated with the corresponding melting points and, in turn, the molecular weight.[56]

Electrochemical Characterization. **TTH** shows four reversible redox couples related to the formation of the radical−anion ($E_{1/2}$ = −1.047 V *vs* Fc/Fc$^+$), anion−anion ($E_{1/2}$ = −1.572 V *vs* Fc/Fc$^+$), radical−cation ($E_{1/2}$ = +1.030 V *vs* Fc/Fc$^+$), and cation−cation ($E_{1/2}$ = +1.278 V *vs* Fc/Fc$^+$) species (Figure 5a). This result is impressive, considering the small dimensions of the *p*QDM derivative.[57−59] The quinoidal stabilization of the diradicaloid determines a slightly reduced electron-acceptor character compared to both **TTM** and **PTH**.[41,60] The electrochemical band gap (Figure 5b) of 2.08 eV resulted to be 0.1 eV smaller than the optical one. The amphoteric redox behavior of **TTH** with four reversible redox couples makes this diradicaloid a promising candidate for energy storage applications[61,62] or air-stable organic field-effect transistors (OFETs),[6,10] especially considering the ambipolar behavior that is usually displayed by singlet diradicaloids.[63]

Spectroscopic Characterization. The absorption spectra of **TTH** in different solvents are reported in Figure 6a, and the main optical properties are summarized in Table 2. The absorption maximum is peaked around 500 nm, slightly depending on the solvent. The molar extinction coefficient in $CHCl_3$ is 48 200 M^{-1} cm^{-1} (502 nm), a value 2 times higher than the one reported for **PTH** (23 150 M^{-1} cm^{-1} at 508 nm).[40] Despite the similar spectral region, **TTH** exhibits a sharper onset and a more symmetric band shape compared to **PTH**. Furthermore, although the transition in the UV is already more intense for **TTH** (13 100 M^{-1} cm^{-1} at 326 nm for **TTH** *vs* 7800 M^{-1} cm^{-1} at 335 nm for **PTH**),[41] such a band is still far less intense compared to that in the visible. As already mentioned, **TTH** showed an intense fluorescence in the deep-red/NIR spectral region, with a broad luminescence peaked at 691 nm in cyclohexane, having a Stokes shift of 193 nm (0.695 eV) and a photoluminescence quantum yield (PLQY) of 0.69 (details in the SI). The emission was bathochromically shifted on increasing the polarity of the solvent, with the emission maximum at 813 nm in benzonitrile (BCN) reaching a Stokes shift value of 307 nm (0.925 eV). This red shift was followed by a slowing of the recombination dynamics (Figure 6b). The PLQY values do not follow the same monotonic trend on increasing the solvent polarity. In fact, extremely high PLQYs were detected in chloroform (PLQY = 0.83) and toluene (PLQY = 0.84), with a maximum of emission around 720 nm. In order to investigate the viscosity-dependent optical properties of **TTH**, different mixtures of hexane and paraffin were employed (Table S5). Upon an increase in viscosity, the absorption (Figure S10) as well as the fluorescence (Figure 6c) maxima were subjected to minor bathochromic shifts. As such, the strong solvent-dependent shifts seen for the fluorescence maxima are exclusively attributed to a polarity-induced solvatochromism. This contrasts the observations made with more extended and flexible derivatives.[65] As the paraffin/hexane ratio increases, fluorescence decay lifetimes are subtly shortened (Figure S11 and Table S5) compared to trends observed when increasing the solvent polarity (Table 2). Interestingly though, the PLQYs show an opposite trend, namely, increasing with decreasing fluorescence lifetime. We rationalize such an observation by a nonradiative deactivation that is hampered at conical

https://doi.org/10.1021/jacs.3c05251
J. Am. Chem. Soc. 2023, 145, 20229−20241

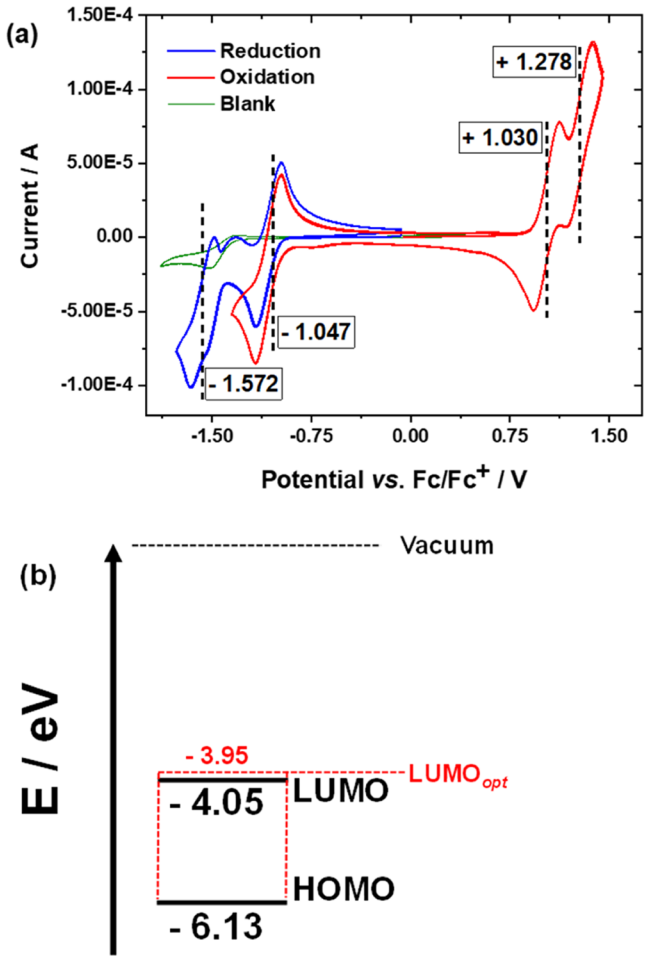

Figure 5. (a) Cyclic voltammogram of a 0.5 mM solution of **TTH** with 0.1 M $N(Bu)_4PF_6$ in CH_2Cl_2 at the scan rate of 0.1 V/s. (b) Representation of the highest occupied molecular orbital (HOMO) and lowest unoccupied molecular orbital (LUMO) calculated through the empirical equations $E_{HOMO} = -[E_{(ox\ vs\ Fc/Fc+)} + 5.1\ V]$ and $E_{LUMO} = -[E_{(red\ vs\ Fc/Fc+)} + 5.1\ V]$.[64] The $LUMO_{opt}$ energy level was estimated as follows: $LUMO_{opt} = HOMO + Eg_{opt}$, in which Eg_{opt} is obtained from the λ_{onset}.

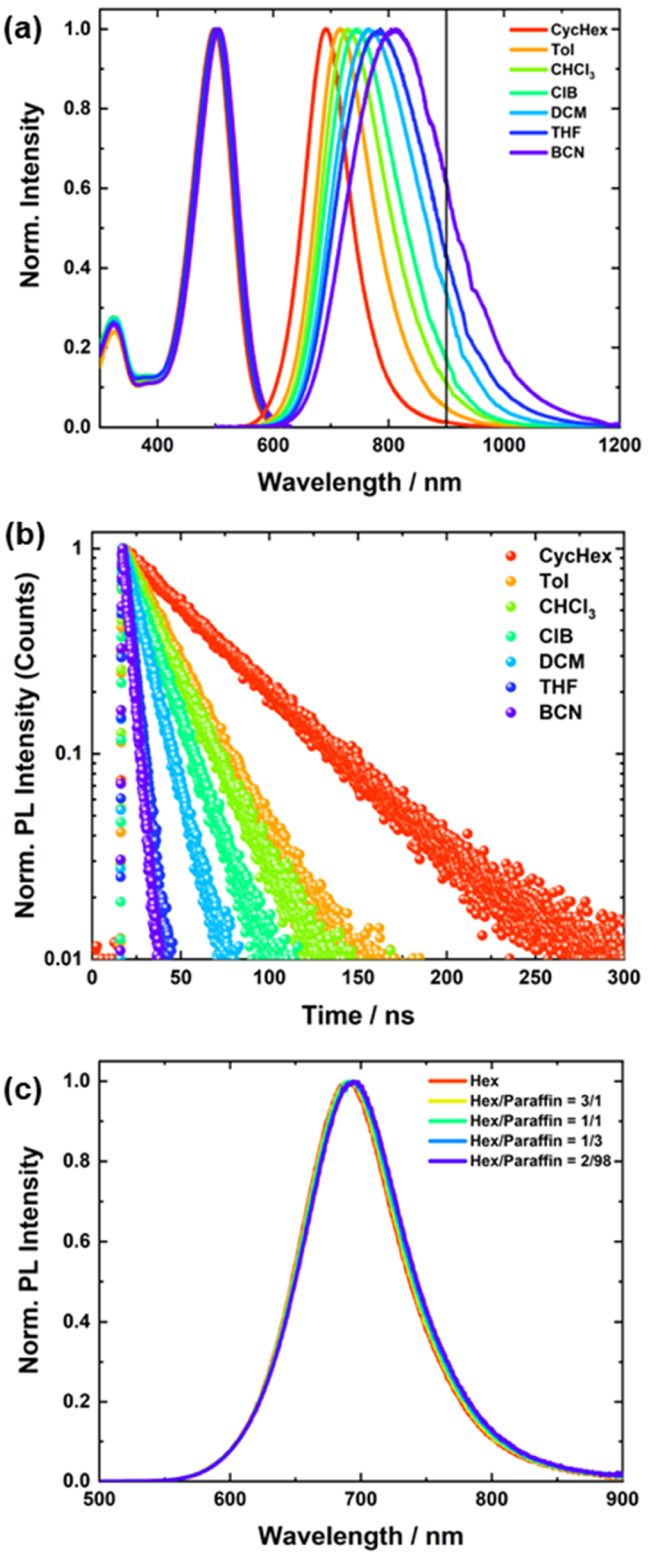

Figure 6. (a) Normalized absorption and emission spectra of **TTH** in different solvents, (b) normalized time-correlated single photon counting (TCSPC) decay profiles of **TTH** measured in different solvents, and (c) normalized emission spectra of **TTH** in different hexane/paraffin mixtures.

intersections between nearby geometries. At the forefront are rotational barriers that rise upon increasing the overall viscosity. At the same time, restrictions of internal motion favor radiative deactivations at certain molecular geometries. This is likely to compensate for the overall singlet excited-state lifetime as it is inversely proportional to the sum of both radiative and nonradiative rate constants. Our considerations contribute to explain the high PLQYs in benzonitrile or even in the solid state and short lifetimes. Relative to THF, the PLQYs are higher and the lifetimes are shorter. In the nonpolar regime, even subtle solvent changes exert sizeable changes on the optical features. A leading example is cyclohexane versus toluene. Even a slightly better stabilization of the zwitterionic character is seen to increase the transition dipole moment and, in turn, to favor the radiative decay. The immediate consequence is a higher PLQY. Interestingly, **TTH** displays an intense fluorescence even in the solid state (Figure S9), unlike what happens with trityl radicals, which suffer a severe aggregation-caused quenching (ACQ).

In fact, thin films of **TTH**, spin-coated (1000 rpm for 60 s) from a chloroform solution (4 mg/mL), show an emission peaked at 703 nm with a PLQY of 0.19 (details in the SI), a value comparable with the state of the art for deep-red/NIR emitters, which makes **TTH** a promising fluorophore for bioimaging and OLEDs.[66,67] Despite the structural analogies

https://doi.org/10.1021/jacs.3c05251
J. Am. Chem. Soc. 2023, 145, 20229−20241

Table 2. Main Optical Properties of TTH in Different Solvents

solvent	λ_{abs} (nm)	ε (M^{-1} cm^{-1})	λ_{em} (nm)	τ^a (ns)	PLQY
CycloHex	498	44 450	691	51.2 ± 0.07	0.69[b]
Hex	496	45 300	691	58.2 ± 0.09	0.62[b]
toluene	503	43 900	716	24.7 ± 0.03	0.84[b]
$CHCl_3$	501	48 200	723	22.6 ± 0.03	0.83[b]
chlorobenzene	505	43 250	745	17.1 ± 0.03	0.53[b]
DCM	502	45 820	765	11.9 ± 0.02	0.48[b]
THF	501	46 060	785	5.3 ± 0.01	0.10[b]
benzonitrile	506	42 600	813	4.2 ± 0.01	0.14[b]
film	513	N.A.	703	4.7 ± 0.2	0.19[c]

[a]The lifetimes have been obtained by best-fitting the decay profiles with a monoexponential function. [b]Values are obtained integrating the emission profile up to ~900 nm. [c]The value is obtained integrating on the whole emission spectrum (up to ~900 nm) obtained by simulating the extension of the experimental data (see the SI).

between **TTH** and **TTM**, no excimer emission was detected in the case of the diradicaloid even when processed as a thin film. The possibility to obtain long-wavelength emission without an extended conjugated system and a remarkable solvatochromism from a nonpolar centrosymmetric derivative opens up new strategies for the molecular design of fluorophores in the NIR region. In fact, similar properties were observed in the case of tetra-aryl *p*QDM derivatives having a strong push−pull character.[44]

Since **TTH** lacks any push−pull feature that might simply explain its emission properties, quantum-chemical calculations aiming to provide new insights about the physical nature of its emitting state were performed.

Quantum-Chemical Calculations. It is well known that in diradicaloids, besides the excited state dominated by the singly excited (SE) H → L configuration (SE state, bright), one distinctive signature is the presence of a "dark" low-lying excited singlet state dominated by the doubly excited (H,H → L,L) electronic configuration (DE state),[68] featuring an ionic (or zwitterionic) character similar to the SE state.[69,70] Such a state, described as two local triplet states coupled as an overall singlet in polyenes,[71,72] has been shown to be the lowest excited state of several conjugated systems displaying a medium to large diradical character[73−75] and can be expected to be a low-lying state for **TTH** also. While the SE state can be correctly captured by time-dependent DFT (TD-DFT) calculations and accounts for the main band in the absorption spectrum (Figure S14), the DE state demands for highly correlated wavefunction methods.[73] Notably, the equilibrium structure of the SE state is markedly diradicaloid, as demonstrated by the elongated CC exocyclic bonds and by the phenyl twisting angles almost identical to those of **TTM** (Figure S15). Furthermore, the H/L gap is strongly reduced compared to the ground-state geometry (dashed double arrows in Figure 7), implying an increasing weight of the H,H → L,L excitation in both ground and excited states, as documented by DFT-MRCI and CASSCF calculations (additional details in the SI). Indeed, at the SE optimized geometry, there is a dramatic difference between the low-lying excited states predicted at the TD-DFT and CASSCF/NEVPT2 levels (Figure 8), with the latter showing a low-lying DE excited state just above the SE (note that the DE state becomes the lowest according to CASPT2 calculations (Figure S16)).

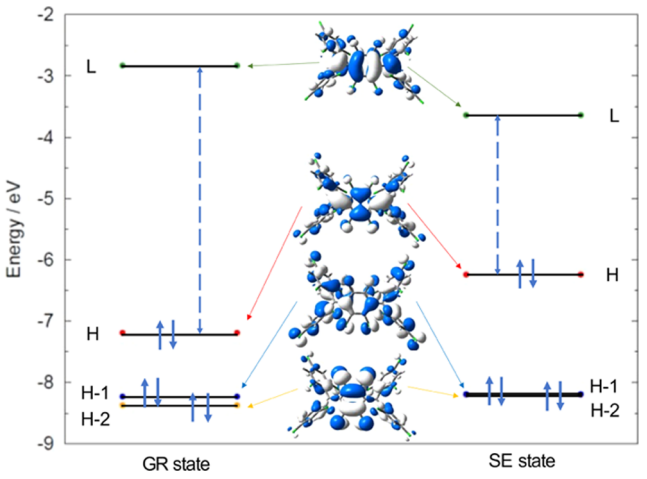

Figure 7. Relevant frontier molecular orbital energies and shapes of **TTH** (M06-2X/def2-SVP+D3 level) at the ground (GR) and singly excited (SE) state optimized geometries showing the remarkable reduction of the H/L gap at the excited-state geometry, implying an energy decrease of the doubly excited configuration and consequently of the DE state.

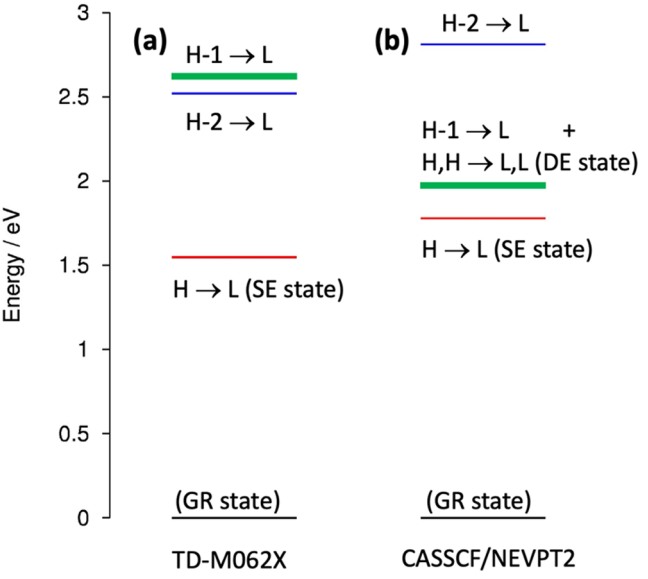

Figure 8. Comparison between low-lying excited states of **TTH** predicted at the equilibrium structure of the SE state: (a) TD-M06-2X/def2-SVP calculations and (b) CASSCF/NEVPT2 calculations. The thick green line is the "dark" state, strongly affected by electron correlation.

Interestingly, the optimized geometry of the DE state displays even more remarkably elongated exocyclic CC bonds than the SE state (Figure S17), implying a small barrier for twisting. To assess the role of twisting around such CC bonds, CASSCF/NEVPT2 calculations were carried out on a smaller *p*QDM derivative, the fully fluorinated tetracyano-quinodimethane **F4TCNQ** (Figure S18), featuring a similar low-lying DE state and documented luminescence properties (maximum value of PLQY = 0.04 in cyclohexane).[76] Twisting around one exocyclic CC bond of **F4TCNQ** generates asymmetric excited conformers featuring non-negligible dipole moments as a result of sudden polarization,[77−79] leading to a solvent-sensitive dipolar structure with red-shifted emission driven by the mixing of the DE and SE ionic states. Calculations show that

https://doi.org/10.1021/jacs.3c05251
J. Am. Chem. Soc. 2023, 145, 20229−20241

such twisted excited states may be preferentially stabilized in polar solvents (Figure S18). At the same time, twisting and SE/DE mixing confer an increased transition dipole moment, thus favoring radiative decay and accounting for the observed luminescence properties. In contrast to the excited state, the ground state is remarkably destabilized for increasing torsional angles, thereby red-shifting the emission and increasing the Stokes shift. These pieces of evidence, applied to **TTH**, suggest that after relaxation to the SE state *via* planarization of the *p*QDM core (Figure 9a) and fast internal conversion to the

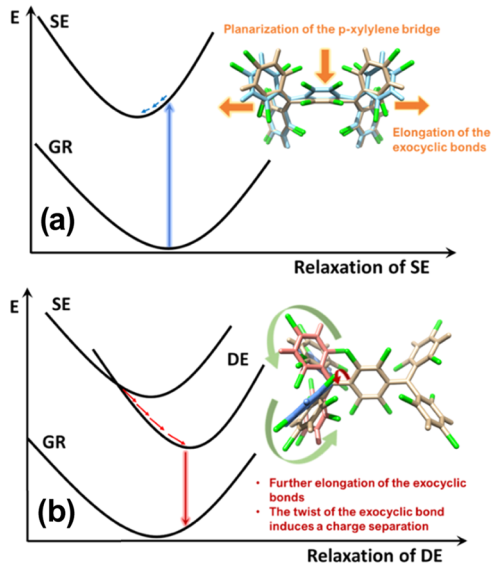

Figure 9. Schematic two-dimensional (2D) representation of the potential energy surfaces (PESs) of the relevant electronic states of **TTH** involved in the photoinduced processes as inferred from CASSCF/NEVPT2 calculations. (a) Main relaxation coordinate in the SE state involving planarization of the *p*QDM core. (b) Subsequent internal conversion to the DE state and relaxation along the CC exocyclic twisting coordinate (red and green arrows in the molecular structure on the right).

lower-lying DE state, the long exocyclic CC bond length afforded in the ionic DE state along with its proximity to the SE state assist the intramolecular torsion, ultimately leading to a charge-separated twisted excited state whose stabilization will be preferential in polar solvents (Figure 9b). Such twisted, charge-separated (zwitterionic) excited states are well known in olefins and justified by sudden polarization,[77−79] a mechanism explaining, in this case, the observed solvent-dependent Stokes shift of **TTH.** Thus, the extreme elongation of the exocyclic CC bonds in the excited DE state of **TTH**, rather unusual for other more extended *p*QDM diradicaloids, makes it comparable to short olefins. While the Herzberg−Teller mechanism has been invoked to explain photoluminescence from the doubly excited "dark" state corresponding to the entangled triplet pair ^{1}(TT) that is the immediate product of singlet fission in oligoacene films[80] (other conjugate systems displaying some diradical character), here we propose that luminescence from the formally "dark" state of the **TTH** diradicaloid is driven by the twisting-induced mixing of SE and DE states.

Transient Absorption (TA) Spectroscopy. We elaborated on the existence and role of the excited DE state by performing fs- and ns-TA spectroscopy by photoexciting close to the absorption band edge at 550 nm. Our fs-TA experiments unambiguously show the involvement of two excited states in the photophysical deactivation cascade (see Figures S19−S25). fs-TA experiments (Figure 10) reveal the primarily populated

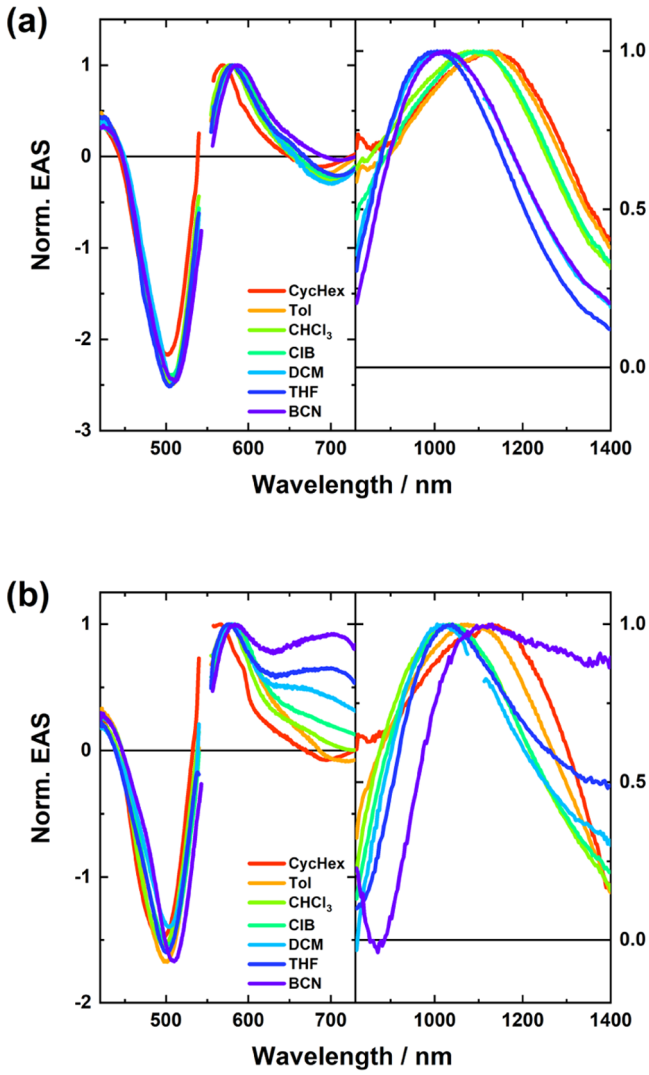

Figure 10. Normalized evolution-associated spectra (EAS) of the deconvoluted species obtained *via* sequential global fitting of the fs-TA raw data measured in different solvents upon photoexcitation at 550 nm. (a) EAS of the excited SE state. (b) EAS of the relaxed excited DE state.

bright singlet excited (SE) state. The spectroscopic signatures thereof include excited-state absorption (ESA) maxima at around 580 nm and in the range from 1000 to 1150 nm. In addition, ground-state bleaching (GSB) at ca. 505 nm and stimulated emission centered around 700 nm were noted. A difference in solvent polarity exerts only a subtle impact on ESA, GSB, and stimulated emission. All of them follow the trend seen in steady-state absorption maxima. Solely, the 1000−1150 nm ESA displays an opposing trend. In stark contrast, the subsequently formed lower-lying excited-state signature, which we assign to the dark DE state, reveals a strong solvent polarity dependence. On one hand, DE exhibits similar solvent-insensitive TA characteristics seen for SE. This speaks for a twisting-induced state mixing between SE and DE and reflects their singlet multiplicities. On the other hand, two additional ESAs evolve at 700 and 1400 nm upon changing the

https://doi.org/10.1021/jacs.3c05251
J. Am. Chem. Soc. 2023, 145, 20229−20241

solvent environment. None of them were present in the TA spectra of SE. Spectro-electrochemical absorption experiments (Figure S26) reveal absorptions, which are due to the one-electron reduced or oxidized form of **TTH**, which are in excellent agreement with these ESAs. This observation supports the notion of a twisted DE with charge-separated character. Stabilization thereof in polar media is derived from an intensity gain of the corresponding ESA. Interestingly, the internal conversion by which SE transforms into DE is found to depend on the solvent viscosity rather than solvent polarity. The corresponding SE lifetimes are obtained from a sequential global fitting procedure and ranged from 2.0 ps for DCM to 8.4 ps for BCN (a summary of all lifetimes is found in Table S9 in the SI). An internal conversion that is viscosity-dependent emphasizes the predicted planarization of the *p*QDM bridge and the simultaneous elongation of the exocyclic CC bonds, which goes ahead of the interstate transition. This is succeeded by a rather slow relaxation along the potential energy surface to reach the minimum of the potential energy surface together, along with a reorganization of the solvent shell. Lifetimes in the range of 100−300 ps indicate a dependence on solvent polarity and viscosity. This is in line with the quantum-mechanically predicted structural rearrangements along the CC exocyclic twisting coordinate, which accompany the transformation toward the relaxed zwitterionic DE (*vide supra*). Its decay exceeds, however, the time window of fs-TA experiments and, in turn, necessitates ns-TA experiments to record the full deactivation dynamics (Figures S27−S34). Importantly, the zwitterionic DE decays monoexponentially on the μs timescale to recover the ground state directly, that is, without the involvement of any other electronic state. The underlying lifetimes show an excellent agreement with the TCSPC results. In other words, the zwitterionic DE is solvatochromatic-emissive. By virtue of solvent stabilization, the energy gap with the electronic ground state as a reference point is reduced. Immediate consequences are steadily shorter lifetimes and lower PLQYs as the solvent polarity is reduced all the way to benzonitrile.

Temperature-Dependent Spectroscopy. To gather additional evidence for a mechanism that is based on twisting zwitterionic DE states, temperature-dependent absorption and fluorescence experiments were performed in 2-methyltetrahydrofuran. With respect to steady-state absorptions of **TTH** (Figure S35), a decrease in temperature down to 80 K induces only subtle shifts. Here, a redistribution of vibrational and rotational energy levels is predominantly operative. This is, however, in stark contrast to the steady-state fluorescence (Figure 11a). When going from room temperature to 160 K, the 775 nm fluorescence maximum shifts bathochromically. Internal motions, which are restricted by the low temperatures, aid in the stabilization of the twisted DE state. Going beyond 160 K, i.e., to 80 K, the trend is reverted and the maximum shifts hypsochromically all the way to 622 nm. Now, even twisting around the elongated exocyclic CC bonds is inhibited. It restricts the formation of a transition dipole moment as a consequence of sudden polarization. Time-resolved fluorescence spectroscopy in the ns regime (Figure 11b,c) independently confirms the aforementioned. At 100 K, a shift of the fluorescence maximum from 630 to 695 nm takes place over the course of excited-state deactivation. A global fit of the data yields three lifetimes: 0.4, 1.5, and 6.5 ns. These results reflect the internal conversion from SE to DE as well as structural relaxations. A considerable change is noted at 80 K.

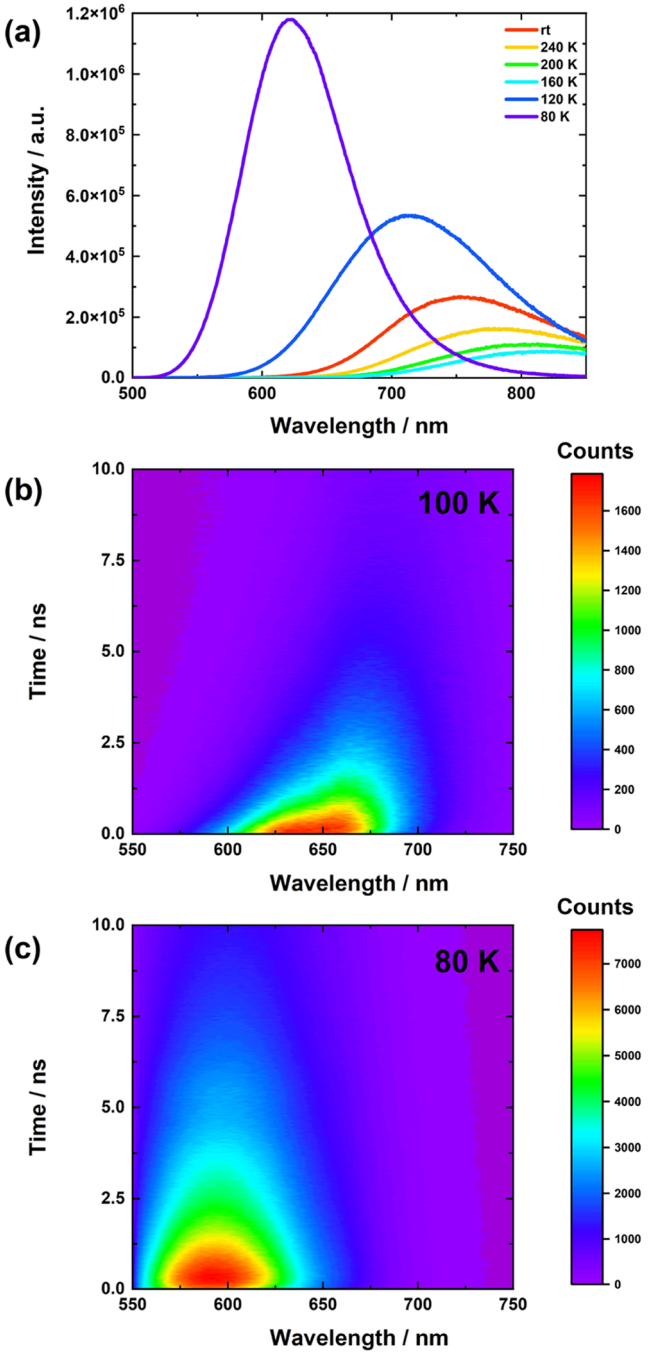

Figure 11. (a) Steady-state fluorescence spectra of **TTH** in 2-methyltetrahydrofuran obtained at various temperatures. (b) ns time-resolved fluorescence plot of **TTH** obtained at 100 K. (c) ns time-resolved fluorescence plot of **TTH** obtained at 80 K.

As a matter of fact, only a minor bathochromic shift from 595 to 600 nm is observed, and two rather than three lifetimes are derived: 2.7 and 11.0 ns. Now, restrictions of internal motions prevent twisting of the exocyclic bonds. This renders a transition toward the zwitterionic DE impossible, and the fluorescence stems exclusively from the unrelaxed/relaxed SE.

CONCLUSIONS

In this work, a comprehensive investigation encompassing synthesis, diverse spectroscopic characterizations, and computational investigations has been used to describe and model, for

https://doi.org/10.1021/jacs.3c05251
J. Am. Chem. Soc. 2023, 145, 20229−20241

the first time, the photoinduced processes leading to the luminescence of **TTH**, a partially chlorinated derivative of the Thiele hydrocarbon. From the synthetic point of view, we demonstrated that polychlorination is a powerful and simple synthetic tool for obtaining neutral, photostable, and inert *p*QDM diradicaloids. Interestingly, **TTH** showed a long-wavelength emission in the deep-red/NIR region without an extended π-system and push−pull character. In addition, extremely high values of PLQY were observed, which is quite uncommon for *p*QDM derivatives, especially considering their solid-state emitting behavior. The large Stokes shift and remarkable solvatochromism of **TTH** luminescence were interpreted with the help of correlated multireference quantum-chemical calculations, indicating that the low-lying DE ionic "dark" state, typically found at low excitation energies in diradicaloids, is responsible for light emission. In **TTH**, such a zwitterionic state becomes the lowest energy excited state and acquires dipole moment and intensity *via* twisting around the elongated exocyclic CC bonds in the excited *p*QDM core with a mechanism involving mixing with the nearby SE state, similar to sudden polarization occurring in olefins. Such a mechanism has been confirmed by fs- and ns-TA measurements. Because the proximity of the SE and DE states can be tuned by chemical substitution, this study paves the way toward modulation of the luminescence properties in diradicaloids by chemical design,[16] making polyhalogenated *p*QDMs extremely interesting open-shell species for photonics and optoelectronics. Interestingly, no solvatochromism, no neat film emission, and lower PLQYs have been detected in the case of a more extended polyhalogenated Müller's hydrocarbon, clearly showing the relevance of the moderate radical character in designing *p*QDM fluorophores.[81]

In addition to their exceptional and unique luminescence properties, **TTH** exhibits four reversible redox couples, which make it suitable for energy storage and electronic applications, or even as a photo-electrocatalytic species for organic synthesis and biomass valorization.[82−84]

■ ASSOCIATED CONTENT

Supporting Information

The Supporting Information is available free of charge at https://pubs.acs.org/doi/10.1021/jacs.3c05251.

Additional experimental details; material and methods; synthetic, spectroscopic, crystallographic, and computational details; NMR spectra for all compounds; TGA data, TCSPC fittings, and fs- and ns-TA spectra in different solvents and temperature-dependent absorption spectra (PDF)

Accession Codes

CCDC 2211356 contains the supplementary crystallographic data for this paper. These data can be obtained free of charge via www.ccdc.cam.ac.uk/data_request/cif, or by emailing data_request@ccdc.cam.ac.uk, or by contacting The Cambridge Crystallographic Data Centre, 12 Union Road, Cambridge CB2 1EZ, UK; fax: +44 1223 336033.

■ AUTHOR INFORMATION

Corresponding Authors

Dirk M. Guldi − *Department of Chemistry and Pharmacy and Interdisciplinary Center for Molecular Materials (ICMM), Friedrich-Alexander-University Erlangen-Nuremberg, 91058 Erlangen, Germany;* orcid.org/0000-0002-3960-1765; Email: dirk.guldi@fau.de

Fabrizia Negri − *Dipartimento di Chimica "Giacomo Ciamician", Università di Bologna and INSTM UdR Bologna, 40126 Bologna, Italy;* orcid.org/0000-0002-0359-0128; Email: fabrizia.negri@unibo.it

Gianluca M. Farinola − *Dipartimento di Chimica, Università degli Studi di Bari Aldo Moro, 70125 Bari, Italy;* orcid.org/0000-0002-1601-2810; Email: gianlucamaria.farinola@uniba.it

Davide Blasi − *Dipartimento di Chimica, Università degli Studi di Bari Aldo Moro, 70125 Bari, Italy;* orcid.org/0000-0002-6887-3364; Email: davide.blasi@uniba.it

Authors

Angela Punzi − *Dipartimento di Chimica, Università degli Studi di Bari Aldo Moro, 70125 Bari, Italy;* orcid.org/0000-0001-5948-6373

Yasi Dai − *Dipartimento di Chimica "Giacomo Ciamician", Università di Bologna and INSTM UdR Bologna, 40126 Bologna, Italy;* orcid.org/0000-0002-4508-7547

Carlo N. Dibenedetto − *Dipartimento di Chimica, Università degli Studi di Bari Aldo Moro, 70125 Bari, Italy; CNR-Istituto per i Processi Chimico Fisici (CNR-IPCF), SS Bari, 70125 Bari, Italy;* orcid.org/0000-0001-9246-2496

Ernesto Mesto − *Dipartimento di Scienze della Terra e Geoambientali, Università degli Studi di Bari Aldo Moro, 70125 Bari, Italy*

Emanuela Schingaro − *Dipartimento di Scienze della Terra e Geoambientali, Università degli Studi di Bari Aldo Moro, 70125 Bari, Italy*

Tobias Ullrich − *Department of Chemistry and Pharmacy and Interdisciplinary Center for Molecular Materials (ICMM), Friedrich-Alexander-University Erlangen-Nuremberg, 91058 Erlangen, Germany*

Marinella Striccoli − *CNR-Istituto per i Processi Chimico Fisici (CNR-IPCF), SS Bari, 70125 Bari, Italy;* orcid.org/0000-0002-5366-691X

Complete contact information is available at: https://pubs.acs.org/10.1021/jacs.3c05251

Author Contributions

[#]A.P. and Y.D. contributed equally to this work.

Funding

Return for Future Innovation (REFIN), an initiative cofunded by the European Union and Apulian region (Italy) through the POR Puglia 2014−2020 (ID grant 2455F798). Ministero dell'Università e della Ricerca (MUR).

Notes

The authors declare no competing financial interest.

■ ACKNOWLEDGMENTS

D.B. and G.M.F. acknowledge Professor Franco Cacialli and Michele Pompilio for their precious help in disclosing the emission properties of **TTH**. Authors acknowledge Dr. Helena Mateos and Professor Rosaria Anna Picca for the fruitful discussion about spectroscopic and electrochemical data. D.B. acknowledges the Return for Future Innovation (REFIN) action for funding. F.N. and Y.D. acknowledge support from "Valutazione della Ricerca di Ateneo" (VRA)—University of Bologna. Y.D. acknowledges Ministero dell'Università e della Ricerca (MUR) for her Ph.D. fellowship.

REFERENCES

(1) Abe, M. Diradicals. *Chem. Rev.* **2013**, *113*, 7011−7088.
(2) Wu, J. *Diradicaloids*; Jenny Standford Publishing, 2022.
(3) Yang, K.; Zhang, X.; Harbuzaru, A.; Wang, L.; Wang, Y.; Koh, C.; Guo, H.; Shi, Y.; Chen, J.; Sun, H.; Feng, K.; Ruiz Delgado, M. C.; Woo, H. Y.; Ortiz, R. P.; Guo, X. Stable Organic Diradicals Based on Fused Quinoidal Oligothiophene Imides with High Electrical Conductivity. *J. Am. Chem. Soc.* **2020**, *142*, 4329−4340.
(4) Kubo, T.; Shimizu, A.; Sakamoto, M.; Uruichi, M.; Yakushi, K.; Nakano, M.; Shiomi, D.; Sato, K.; Takui, T.; Morita, Y.; Nakasuji, K. Synthesis, Intermolecular Interaction, and Semiconductive Behavior of a Delocalized Singlet Biradical Hydrocarbon. *Angew. Chem., Int. Ed.* **2005**, *44*, 6564−6568.
(5) Casado, J.; Mori, S.; Moles Quintero, S.; Tabaka, N.; Kishi, R.; González Núñez, R.; Harbuzaru, A.; Ponce, R.; Marin Beloqui, J.; Suzuki, S.; kitamura, C.; Gómez, C.; Dai, Y.; Negri, F.; Nakano, M.; Kato, S. Medium Diradical Character, Small Hole and Electron Reorganization Energies and Ambipolar Transistors in Difluorenoheteroles. *Angew. Chem., Int. Ed.* **2022**, No. e202206680.
(6) Zong, C.; Zhu, X.; Xu, Z.; Zhang, L.; Xu, J.; Guo, J.; Xiang, Q.; Zeng, Z.; Hu, W.; Wu, J.; Li, R.; Sun, Z. Isomeric Dibenzoheptazethrenes for Air-Stable Organic Field-Effect Transistors. *Angew. Chem.* **2021**, *133*, 16366−16372.
(7) Brosius, V.; Weigold, S.; Hippchen, N.; Rominger, F.; Freudenberg, J.; Bunz, U. H. F. Diindenopyrazines: Electron-Deficient Arenes. *Chem.—Eur. J.* **2021**, *27*, 10001−10005.
(8) Koike, H.; Chikamatsu, M.; Azumi, R.; Tsutsumi, J.; Ogawa, K.; Yamane, W.; Nishiuchi, T.; Kubo, T.; Hasegawa, T.; Kanai, K. Stable Delocalized Singlet Biradical Hydrocarbon for Organic Field-Effect Transistors. *Adv. Funct. Mater.* **2016**, *26*, 277−283.
(9) Chen, J. F.; Tian, G.; Liu, K.; Zhang, N.; Wang, N.; Yin, X.; Chen, P. Pillar[5]Arene-Based Neutral Radicals with Doublet Red Emissions and Stable Chiroptical Properties. *Org. Lett.* **2022**, *24*, 1935−1940.
(10) Messelberger, J.; Grünwald, A.; Pinter, P.; Hansmann, M. M.; Munz, D. Carbene Derived Diradicaloids-Building Blocks for Singlet Fission? *Chem. Sci.* **2018**, *9*, 6107−6117.
(11) Varnavski, O.; Abeyasinghe, N.; Aragó, J.; Serrano-Pérez, J. J.; Ortí, E.; López Navarrete, J. T.; Takimiya, K.; Casanova, D.; Casado, J.; Goodson, T. High Yield Ultrafast Intramolecular Singlet Exciton Fission in a Quinoidal Bithiophene. *J. Phys. Chem. Lett.* **2015**, *6*, 1375−1384.
(12) Kamada, K.; Fuku-En, S. I.; Minamide, S.; Ohta, K.; Kishi, R.; Nakano, M.; Matsuzaki, H.; Okamoto, H.; Higashikawa, H.; Inoue, K.; Kojima, S.; Yamamoto, Y. Impact of Diradical Character on Two-Photon Absorption: Bis(Acridine) Dimers Synthesized from an Allenic Precursor. *J. Am. Chem. Soc.* **2013**, *135*, 232−241.
(13) Sun, Z.; Ye, Q.; Chi, C.; Wu, J. Low Band Gap Polycyclic Hydrocarbons: From Closed-Shell near Infrared Dyes and Semiconductors to Open-Shell Radicals. *Chem. Soc. Rev.* **2012**, *41*, 7857−7889.
(14) Wang, L.; Zhang, T.-S.; Tian, X.; Guo, S.; Wang, H.; Cui, G.; Fang, W.-H.; Fu, H.; Yao, J. Conformational Distortion-Harnessed Singlet Fission Dynamics in Thienoquinoid: Rapid Generation and Subsequent Annihilation of Multiexciton Dark State. *J. Mater. Chem. C* **2022**, *10*, 4268−4275.
(15) Lukman, S.; Richter, J. M.; Yang, L.; Hu, P.; Wu, J.; Greenham, N. C.; Musser, A. J. Efficient Singlet Fission and Triplet-Pair Emission in a Family of Zethrene Diradicaloids. *J. Am. Chem. Soc.* **2017**, *139*, 18376−18385.
(16) Ren, L.; Liu, F.; Shen, X.; Zhang, C.; Yi, Y.; Zhu, X. Developing Quinoidal Fluorophores with Unusually Strong Red/Near-Infrared Emission. *J. Am. Chem. Soc.* **2015**, *137*, 11294−11302.
(17) Thiele, J.; Balhorn, H. Ueber Einen Chinoiden Kohlenwasserstoff. *Ber. Dtsch. Chem. Ges.* **1904**, *37*, 1463−1470.
(18) Montgomery, L. K.; Huffman, J. C.; Jurczak, E. A.; Grendze, M. P. The Molecular Structures of Thiele's and Chichibabin's Hydrocarbons. *J. Am. Chem. Soc.* **1986**, *108*, 6004−6011.
(19) Yamaguchi, K. The Electronic Structures of Biradicals in the Unrestricted Hartree-Fock Approximation. *Chem. Phys. Lett.* **1975**, *33*, 330−335.
(20) Maiti, A.; Stubbe, J.; Neuman, N. I.; Kalita, P.; Duari, P.; Schulzke, C.; Chandrasekhar, V.; Sarkar, B.; Jana, A. CAAC-Based Thiele and Schlenk Hydrocarbons. *Angew. Chem., Int. Ed.* **2020**, *59*, 6729−6734.
(21) Maiti, A.; Chandra, S.; Sarkar, B.; Jana, A. Acyclic Diaminocarbene-Based Thiele, Chichibabin, and Müller Hydrocarbons. *Chem. Sci.* **2020**, *11*, 11827−11833.
(22) Maiti, A.; Zhang, F.; Krummenacher, I.; Bhattacharyya, M.; Mehta, S.; Moos, M.; Lambert, C.; Engels, B.; Mondal, A.; Braunschweig, H.; Ravat, P.; Jana, A. Anionic Boron- And Carbon-Based Hetero-Diradicaloids Spanned by a p-Phenylene Bridge. *J. Am. Chem. Soc.* **2021**, *143*, 3687−3692.
(23) Tan, G.; Wang, X. Isolable Bis(Triarylamine) Dications: Analogues of Thiele's, Chichibabin's, and Müller's Hydrocarbons. *Acc. Chem. Res.* **2017**, *50*, 1997−2006.
(24) Jiménez, V. G.; Mayorga-Burrezo, P.; Blanco, V.; Lloveras, V.; Gómez-García, C. J.; Šolomek, T.; Cuerva, J. M.; Veciana, J.; Campaña, A. G. Dibenzocycloheptatriene as End-Group of Thiele and Tetrabenzo-Chichibabin Hydrocarbons. *Chem. Commun.* **2020**, *56*, 12813−12816.
(25) Petakova, V.; Nedyalkova, M.; Stoycheva, J.; Tadjer, A.; Romanova, J. The Interplay between Diradical Character and Stability in Organic Molecules. *Symmetry* **2021**, *13*, No. 1448.
(26) Matsuoka, R.; Mizuno, A.; Mibu, T.; Kusamoto, T. Luminescence of Doublet Molecular Systems. *Coord. Chem. Rev.* **2022**, *467*, No. 214616.
(27) Ratera, I.; Marcen, S.; Montant, S.; Ruiz Molina, D.; Rovira, C.; Veciana, J.; Létard, J. F.; Freysz, E. Nonlinear Optical Properties of Polychlorotriphenylmethyl Radicals: Towards the Design of "super-Octupolar" Molecules. *Chem. Phys. Lett.* **2002**, *363*, 245−251.
(28) Hattori, Y.; Michail, E.; Schmiedel, A.; Moos, M.; Holzapfel, M.; Krummenacher, I.; Braunschweig, H.; Müller, U.; Pflaum, J.; Lambert, C. Luminescent Mono-, Di-, and Triradicals: Bridging Polychlorinated Triarylmethyl Radicals by Triarylamines and Triarylboranes. *Chem.—Eur. J.* **2019**, *25*, 15463−15471.
(29) Jin, Q.; Chen, S.; Sang, Y.; Guo, H.; Dong, S.; Han, J.; Chen, W.; Yang, X.; Li, F.; Duan, P. Circularly Polarized Luminescence of Achiral Open-Shell π-Radicals. *Chem. Commun.* **2019**, *55*, 6583−6586.
(30) Mayorga Burrezo, P.; Jiménez, V. G.; Blasi, D.; Ratera, I.; Campaña, A. G.; Veciana, J. Organic Free Radicals as Circularly Polarized Luminescence Emitters. *Angew. Chem., Int. Ed.* **2019**, *58*, 16282−16288.
(31) Mayorga-Burrezo, P.; Jiménez, V. G.; Blasi, D.; Parella, T.; Ratera, I.; Campaña, A. G.; Veciana, J. An Enantiopure Propeller-Like Trityl-Brominated Radical: Bringing Together a High Racemization Barrier and an Efficient Circularly Polarized Luminescent Magnetic Emitter. *Chem.—Eur. J.* **2020**, *26*, 3776−3781.
(32) Kato, K.; Kimura, S.; Kusamoto, T.; Nishihara, H.; Teki, Y. Luminescent Radical-Excimer: Excited-State Dynamics of Luminescent Radicals in Doped Host Crystals. *Angew. Chem., Int. Ed.* **2019**, *58*, 2606−2611.
(33) Kimura, S.; Kimura, S.; Kato, K.; Teki, Y.; Nishihara, H.; Kusamoto, T. A Ground-State-Dominated Magnetic Field Effect on the Luminescence of Stable Organic Radicals. *Chem. Sci.* **2021**, *12*, 2025−2029.
(34) Abdurahman, A.; Hele, T. J. H.; Gu, Q.; Zhang, J.; Peng, Q.; Zhang, M.; Friend, R. H.; Li, F.; Evans, E. W. Understanding the Luminescent Nature of Organic Radicals for Efficient Doublet Emitters and Pure-Red Light-Emitting Diodes. *Nat. Mater.* **2020**, *19*, 1224−1229.
(35) Peng, Q.; Obolda, A.; Zhang, M.; Li, F. Organic Light-Emitting Diodes Using a Neutral π Radical as Emitter: The Emission from a Doublet. *Angew. Chem., Int. Ed.* **2015**, *54*, 7091−7095.
(36) Blasi, D.; Nikolaidou, D. M.; Terenziani, F.; Ratera, I.; Veciana, J. Excimers from Stable and Persistent Supramolecular Radical-Pairs

https://doi.org/10.1021/jacs.3c05251
J. Am. Chem. Soc. 2023, 145, 20229−20241

in Red/NIR-Emitting Organic Nanoparticles and Polymeric Films. *Phys. Chem. Chem. Phys.* **2017**, *19*, 9313−9319.
(37) Ai, X.; Evans, E. W.; Dong, S.; Gillett, A. J.; Guo, H.; Chen, Y.; Hele, T. J. H.; Friend, R. H.; Li, F. Efficient Radical-Based Light-Emitting Diodes with Doublet Emission. *Nature* **2018**, *563*, 536−540.
(38) Ratera, I.; Veciana, J. Playing with Organic Radicals as Building Blocks for Functional Molecular Materials. *Chem. Soc. Rev.* **2012**, *41*, 303−349.
(39) Veciana, J.; Rovira, C.; Armet, O.; Domingo, V. M.; Crespo, M. I.; Palacio, F. Stable Triplets and Quartets from Carbon Centered Polyradicals. *Mol. Cryst. Liq. Cryst. Incorporating Nonlinear Opt.* **1989**, *176*, 77−84.
(40) Castañer, J.; Riera, J. Highly Crowded Perchloropolyphenyl-p-Xylylenes with Exceptional Thermal Stability. *J. Org. Chem.* **1991**, *56*, 5445−5448.
(41) Domingo, V. M.; Castañer, J.; Riera, J.; Brillas, E.; Molins, E.; Martinez, B.; Knight, B. Inert Carbon Free Radicals. 14. Synthesis, Isolation, and Properties of Two Strongly π-π Interacting Mixed-Valence Compounds: The Perchloro-4,4′-Ethynylenebis-(Triphenylmethyl) Anion Radical Potassium (18-Crown-6) Salt and the Perchloro-α,α,A′,A′-Tetraphen. *Chem. Mater.* **1997**, *9*, 1620−1629.
(42) Guo, H.; Peng, Q.; Chen, X. K.; Gu, Q.; Dong, S.; Evans, E. W.; Gillett, A. J.; Ai, X.; Zhang, M.; Credgington, D.; Coropceanu, V.; Friend, R. H.; Brédas, J. L.; Li, F. High Stability and Luminescence Efficiency in Donor−Acceptor Neutral Radicals Not Following the Aufbau Principle. *Nat. Mater.* **2019**, *18*, 977−984.
(43) Gopalakrishna, T. Y.; Zeng, W.; Lu, X.; Wu, J. From Open-Shell Singlet Diradicaloids to Polyradicaloids. *Chem. Commun.* **2018**, *54*, 2186−2199.
(44) Okamoto, Y.; Tanioka, M.; Muranaka, A.; Miyamoto, K.; Aoyama, T.; Ouyang, X.; Kamino, S.; Sawada, D.; Uchiyama, M. Stable Thiele's Hydrocarbon Derivatives Exhibiting Near-Infrared Absorption/Emission and Two-Step Electrochromism. *J. Am. Chem. Soc.* **2018**, *140*, 17857−17861.
(45) Ullrich, T.; Pinter, P.; Messelberger, J.; Haines, P.; Kaur, R.; Hansmann, M. M.; Munz, D.; Guldi, D. M. Singlet Fission in Carbene-Derived Diradicaloids. *Angew. Chem., Int. Ed.* **2020**, *59*, 7906−7914.
(46) Wehrmann, C. M.; Imran, M.; Pointer, C.; Fredin, L. A.; Young, E. R.; Chen, M. S. Spin Multiplicity Effects in Doublet: Versus Singlet Emission: The Photophysical Consequences of a Single Electron. *Chem. Sci.* **2020**, *11*, 10212−10219.
(47) Ishigaki, Y.; Hashimoto, T.; Sugawara, K.; Suzuki, S.; Suzuki, T. Switching of Redox Properties Triggered by a Thermal Equilibrium between Closed-Shell Folded and Open-Shell Twisted Species. *Angew. Chem., Int. Ed.* **2020**, *59*, 6581−6584.
(48) Li, K.; Xu, Z.; Xu, J.; Weng, T.; Chen, X.; Sato, S.; Wu, J.; Sun, Z. Overcrowded Ethylene-Bridged Nanohoop Dimers: Regioselective Synthesis, Multiconfigurational Electronic States, and Global Hückel/Möbius Aromaticity. *J. Am. Chem. Soc.* **2021**, *143*, 20419−20430.
(49) Nishiuchi, T.; Aibara, S.; Sato, H.; Kubo, T. Synthesis of π-Extended Thiele's and Chichibabin's Hydrocarbons and Effect of the π-Congestion on Conformations and Electronic States. *J. Am. Chem. Soc.* **2022**, *144*, 7479−7488.
(50) The Reaction Was Previously Tested Using Just 6 equiv of TBAOH. The Amount of Monoradical Seams to Be Independent by the Excess of Base Used for the Formation of Cabanion.
(51) Castellanos, S.; Velasco, D.; López-Calahorra, F.; Brillas, E.; Julia, L. Taking Advantage of the Radical Character of Tris(2,4,6-Trichlorophenyl) Methyl to Synthesize New Paramagnetic Glassy Molecular Materials. *J. Org. Chem.* **2008**, *73*, 3759−3767.
(52) Heckmann, A.; Dümmler, S.; Pauli, J.; Margraf, M.; Köhler, J.; Stich, D.; Lambert, C.; Fischer, I.; Resch-Genger, U. Highly Fluorescent Open-Shell NIR Dyes: The Time-Dependence of Back Electron Transfer in Triarylamine-Perchlorotriphenylmethyl Radicals. *J. Phys. Chem. C* **2009**, *113*, 20958−20966.
(53) Zhou, H.; Wu, S.; Duan, Y.; Gao, F.; Pan, Q.; Kan, Y.; Su, Z. A Theoretical Study on the Donor Ability Better Organic Luminescent Materials †. *New J. Chem.* **2022**, 16325−16332.
(54) Armet, O.; Veciana, J.; Rovira, C.; Riera, J.; Castañer, J.; Molins, E.; Rius, J.; Miravitlles, C.; Olivella, S.; Brichfeus, J. Inert Carbon Free Radicals. 8. Polychlorotriphenylmethyl Radicals. Synthesis, Structure, and Spin-Density Distribution. *J. Phys. Chem. A* **1987**, *91*, 5608−5616.
(55) Souto, M.; Cui, H.; Peña-Álvarez, M.; Baonza, V. G.; Jeschke, H. O.; Tomic, M.; Valentí, R.; Blasi, D.; Ratera, I.; Rovira, C.; Veciana, J. Pressure-Induced Conductivity in a Neutral Nonplanar Spin-Localized Radical. *J. Am. Chem. Soc.* **2016**, *138*, 11517−11525.
(56) Ballester, M.; Castañer, J.; Riera, J.; Pujadas, J.; Armet, O.; Onrubia, C.; Rio, J. A. Inert Carbon Free Radicals. 5. Perchloro-9-Phenylfluorenyl Radical Series. *J. Org. Chem.* **1984**, *49*, 770−778.
(57) Dong, S.; Gopalakrishna, T. Y.; Han, Y.; Phan, H.; Tao, T.; Ni, Y.; Liu, G.; Chi, C. Extended Bis(Anthraoxa)Quinodimethanes with Nine and Ten Consecutively Fused Six-Membered Rings: Neutral Diradicaloids and Charged Diradical Dianions/Dications. *J. Am. Chem. Soc.* **2019**, *141*, 62−66.
(58) Jiang, Q.; Han, Y.; Zou, Y.; Phan, H.; Yuan, L.; Herng, T. S.; Ding, J.; Chi, C. S-Shaped Para-Quinodimethane-Embedded Double [6]Helicene and Its Charged Species Showing Open-Shell Diradical Character. *Chem.—Eur. J.* **2020**, *26*, 15613−15622.
(59) Dong, S.; Gopalakrishna, T. Y.; Han, Y.; Chi, C. Cyclobis(7,8-(Para -quinodimethane)-4,4′-triphenylamine) and Its Cationic Species Showing Annulene-Like Global (Anti)Aromaticity. *Angew. Chem.* **2019**, *131*, 11868−11872.
(60) Tesio, A. Y.; Blasi, D.; Olivares-Marín, M.; Ratera, I.; Tonti, D.; Veciana, J. Organic Radicals for the Enhancement of Oxygen Reduction Reaction in Li-O2 Batteries. *Chem. Commun.* **2015**, *51*, 17623−17626.
(61) Morita, Y.; Nishida, S.; Murata, T.; Moriguchi, M.; Ueda, A.; Satoh, M.; Arifuku, K.; Sato, K.; Takui, T. Organic Tailored Batteries Materials Using Stable Open-Shell Molecules with Degenerate Frontier Orbitals. *Nat. Mater.* **2011**, *10*, 947−951.
(62) Majewski, M. A.; Chmielewski, P. J.; Chien, A.; Hong, Y.; Lis, T.; Witwicki, M.; Kim, D.; Zimmerman, P. M.; Stępień, M. 5,10-Dimesityldiindeno[1,2-a:2′,1′-i]Phenanthrene: A Stable Biradicaloid Derived from Chichibabin's Hydrocarbon. *Chem. Sci.* **2019**, *10*, 3413−3420.
(63) Huang, Y.; Egap, E. Open-Shell Organic Semiconductors: An Emerging Class of Materials with Novel Properties. *Polym. J.* **2018**, *50*, 603−614.
(64) Cardona, C. M.; Li, W.; Kaifer, A. E.; Stockdale, D.; Bazan, G. C. Electrochemical Considerations for Determining Absolute Frontier Orbital Energy Levels of Conjugated Polymers for Solar Cell Applications. *Adv. Mater.* **2011**, *23*, 2367−2371.
(65) Kotani, R.; Sotome, H.; Okajima, H.; Yokoyama, S.; Nakaike, Y.; Kashiwagi, A.; Mori, C.; Nakada, Y.; Yamaguchi, S.; Osuka, A.; Sakamoto, A.; Miyasaka, H.; Saito, S. Flapping Viscosity Probe That Shows Polarity-Independent Ratiometric Fluorescence. *J. Mater. Chem. C* **2017**, *5*, 5248−5256.
(66) Tu, L.; Xie, Y.; Li, Z.; Tang, B. Aggregation-induced Emission: Red and Near-infrared Organic Light-emitting Diodes. *SmartMat* **2021**, *2*, 326−346.
(67) Jackson, C. T.; Jeong, S.; Dorlhiac, G. F.; Landry, M. P. Advances in Engineering Near-Infrared Luminescent Materials. *iScience* **2021**, *24*, No. 102156.
(68) Bonačić-Koutecký, V.; Koutecký, J.; Michl, J. Neutral and Charged Biradicals, Zwitterions, Funnels in S1, and Proton Translocation: Their Role in Photochemistry, Photophysics, and Vision. *Angew. Chem., Int. Ed.* **1987**, *26*, 170−189.
(69) Nakano, M. Open-Shell-Character-Based Molecular Design Principles: Applications to Nonlinear Optics and Singlet Fission. *Chem. Rec.* **2017**, *17*, 27−62.
(70) Stuyver, T.; Chen, B.; Zeng, T.; Geerlings, P.; De Proft, F.; Hoffmann, R. Do Diradicals Behave like Radicals. *Chem. Rev.* **2019**, *119*, 11291−11351.

https://doi.org/10.1021/jacs.3c05251
J. Am. Chem. Soc. 2023, 145, 20229−20241

(71) Kim, H.; Zimmerman, P. M. Coupled Double Triplet State in Singlet Fission. *Phys. Chem. Chem. Phys.* **2018**, *20*, 30083−30094.
(72) Sandoval-Salinas, M. E.; Casanova, D. The Doubly Excited State in Singlet Fission. *ChemPhotoChem* **2021**, *5*, 282−293.
(73) Di Motta, S.; Negri, F.; Fazzi, D.; Castiglioni, C.; Canesi, E. V. Biradicaloid and Polyenic Character of Quinoidal Oligothiophenes Revealed by the Presence of a Low-Lying Double-Exciton State. *J. Phys. Chem. Lett.* **2010**, *1*, 3334−3339.
(74) González-Cano, R. C.; Di Motta, S.; Zhu, X.; López Navarrete, J. T.; Tsuji, H.; Nakamura, E.; Negri, F.; Casado, J. Carbon-Bridged Phenylene-Vinylenes: On the Common Diradicaloid Origin of Their Photonic and Chemical Properties. *J. Phys. Chem. C* **2017**, *121*, 23141−23148.
(75) Negri, F.; Canola, S.; Dai, Y. Spectroscopy of Open-Shell Singlet Ground-State Diradicaloids: A Computational Perspective. In *Diradicaloids*; Wu, J., Ed.; Jenny Stanford Publishing: New York, NY, 2022; pp 145−179.
(76) Torii, Y.; Niioka, Y.; Syundo, K.; Kashiwagi, D.; Iimori, T. Solvatochromism of Fluorescence and the Excited State of 2,3,5,6-Tetrafluoro-7,7,8,8-Tetracyanoquinodimethane. *J. Lumin.* **2022**, *241*, No. 118503.
(77) Koutecky, J.; Bonačič-Koutecký, V.; Čížek, J.; Döhnert, D. Nature of the "Sudden Polarization" Effect and Its Role in Photochemistry. *Int. J. Quantum Chem.* **2009**, *14*, 357−369.
(78) Filatov, M.; Lee, S.; Choi, C. H. Description of Sudden Polarization in the Excited Electronic States with an Ensemble Density Functional Theory Method. *J. Chem. Theory Comput.* **2021**, *17*, 5123−5139.
(79) Bersuker, I. B. Jahn-Teller and Pseudo-Jahn-Teller Effects: From Particular Features to General Tools in Exploring Molecular and Solid State Properties. *Chem. Rev.* **2021**, *121*, 1463−1512.
(80) Yong, C. K.; Musser, A. J.; Bayliss, S. L.; Lukman, S.; Tamura, H.; Bubnova, O.; Hallani, R. K.; Meneau, A.; Resel, R.; Maruyama, M.; Hotta, S.; Herz, L. M.; Beljonne, D.; Anthony, J. E.; Clark, J.; Sirringhaus, H. The Entangled Triplet Pair State in Acene and Heteroacene Materials. *Nat. Commun.* **2017**, *8*, No. 15953.
(81) Abdurahman, A.; Wang, J.; Zhao, Y.; Li, P.; Shen, L.; Peng, Q. A Highly Stable Organic Luminescent Diradical. *Angew. Chem., Int. Ed.* **2023**, No. 210023.
(82) Huang, H.; Strater, Z. M.; Rauch, M.; Shee, J.; Sisto, T. J.; Nuckolls, C.; Lambert, T. H. Electrophotocatalysis with a Trisaminocyclopropenium Radical Dication. *Angew. Chem., Int. Ed.* **2019**, *58*, 13318−13322.
(83) Naidu, V. R.; Ni, S.; Franzén, J. The Carbocation: A Forgotten Lewis Acid Catalyst. *ChemCatChem* **2015**, *7*, 1896−1905.
(84) Nguyen, S. T.; Murray, P. R. D.; Knowles, R. R. Light-Driven Depolymerization of Native Lignin Enabled by Proton-Coupled Electron Transfer. *ACS Catal.* **2020**, *10*, 800−805.

NOTE ADDED AFTER ASAP PUBLICATION

This paper was published on September 6, 2023. Due to production error, an incorrect Supporting Information file was published. The corrected version was posted on September 6, 2023.

https://doi.org/10.1021/jacs.3c05251
J. Am. Chem. Soc. 2023, 145, 20229−20241